Three-dimensional atom probe analysis of boron segregation at austenite grain boundary in a low carbon steel - Effects of boundary misorientation and quenching temperature

Three-dimensional atom probe analysis of boron segregation at austenite grain boundary in a low carbon steel - effects of boundary misorientation and quenching temperature

Goro Miyamoto[a,*], Ai Goto[b], Naoki Takayama[c], Tadashi Furuhara[a]

[a.] Institute for Materials Research, Tohoku University, 2-1-1 Katahira, Aoba-ku, Sendai 980-8577 Japan.

[b.] Formerly graduate student, Department of Metallurgy, Tohoku University, currently at Nippon Steel Sumitomo Metals

[c.] JFE Steel Corporation, 1-1 Minamiwatarida-cho, Kawasaki-Ku, Kawasaki, 210-0855, Japan.

* Corresponding author

Email: miyamoto@imr.tohoku.ac.jp(G.M.)

Segregation of boron at random austenite grain boundaries with known misorientation angle in a boron-added low carbon steel quenched from austenite state at different temperatures was investigated quantitatively using three-dimensional atom probe. Boron segregation is reduced at low angle boundaries or low quenching temperatures. The latter result indicates that non-equilibrium boron segregation plays an important role and is enhanced at higher quenching temperature due to more excess vacancies and longer diffusion distance during quenching from higher temperature.

Addition of small amount of boron (B) can significantly improve hardenability of steels and are widely used in the production of high strength thick steel plates having martensite or bainite structures [1]. It has been considered that segregation of B atoms at austenite grain boundary lowers austenite grain boundary energy and delays nucleation of ferrite at austenite grain boundary [2]. Therefore, understanding of B segregation at austenite grain boundary is a key issue in microstructure control by B addition.

B segregation at austenite grain boundaries has been investigated extensively using secondary ion mass spectroscopy (SIMS), one dimensional atom probe tomography (APT) and alpha-particle track etching (ATE) [3-6]. Those studies have revealed that B segregation depends on a temperature before cooling, a cooling rate and other alloying elements and also influenced by precipitation of borides. One peculiar behavior of B segregation detected by ATE is a reduction of B segregation after cooling from lower temperature [6]. This temperature dependency, inconsistent with equilibrium segregation predicted by the McLean model, was understood in terms of non-equilibrium segregation where annihilation of excess vacancies at austenite grain boundaries induces a vacancy-B complex flow

toward grain boundaries and results in accumulation of B atoms at grain boundaries [7]. However, spatial resolution of ATE is far poorer compared with a grain boundary thickness and is not sufficient to investigate B segregation quantitatively.

Recently, scanning transmission electron microscopy equipped with electron energy loss spectroscopy (STEM-EELS) or three dimensional atom probe (3DAP) have been applied to quantitatively measure B segregation at austenite grain boundaries [8-10]. Takahashi et al. [10] systematically investigated effects of cooling rates from 950°C on B segregation using 3DAP and found that B segregation increases at slower cooling rate if boride precipitation is avoided. They also reported that a diffusion limited equilibrium segregation model can reproduce observed B segregation and concluded that an effect of non-equilibrium B segregation is small in cooling from 950°C due to low vacancy concentration at such low temperature. However, different B segregation behavior is expected in cooling from higher temperature where vacancy concentration is high although effects of a temperature before cooling on B segregation is unknown.

Furthermore, as summarized in a textbook [11], boundary segregation of solute strongly depends on grain boundary character such as misorientation angle and boundary plane. Recent correlative 3DAP and TEM analyses of carbon (C) segregation to ferrite boundaries clearly show that segregation behavior to low angle boundaries differs significantly from that for high angle grain boundaries [12]. However, there is almost no investigation on boundary character dependence of B segregation.

Therefore, in this study, we aim to investigate B segregation at austenite grain boundaries in the specimens quenched from various temperatures using 3DAP together with characterization of austenite grain boundaries in order to clarify B segregation mechanism.

Fe-0.19C-1.99Mn-0.015Ti-0.0018N-11ppmB (mass%) alloy was used in this study. Ti is added to scavenge nitrogen in order to prevent from consumption of B by the formation of BN. After an annealing at 1150 °C for 24 h to homogenize Mn segregation, 3×5×10mm^3 rectangular specimens were cut, and heat-treated in three different conditions as shown in Fig. 1(a). One specimen was austenitized at 1200 °C for 10 min, and subsequently quenched into water. In order to investigate effects of quenching temperature on B segregation without changing a austenite grain size, two-steps heat treatment was conducted; the specimens were held at 1050 °C or 900 °C following to austenitization at 1200 °C, and water-quenched as shown in Fig. 1(a). Longer annealing periods in the second step were applied to ensure similar diffusion distances for all the annealing temperatures for segregation. Those specimens are denoted as Q1200°C, Q1050°C and Q900°C, respectively. Average prior austenite grain size is about 80μm in the three specimens. Average cooling rates between 1100 to 400°C during water-quenching were measured several times by a thermocouple welded inside of a rectangular specimen and vary from 980 to 1340 °C/s.

Orientation of martensite was measured by electron backscattering diffraction (EBSD: OIM ver. 7 produced by EDAX) equipped with a field emission scanning electron microscope (SEM : JSM-7001F produced by JEOL and operated at 15kV) and orientation of prior austenite was reconstructed using a method developed by some of the present authors as shown in Figs. 1(b) and (c) [13]. Then, several needle specimens for 3DAP measurement were prepared from multiple prior austenite grain boundaries (PAGBs) with known misorientations using focused ion beam (FIB) method. It should be noted that only random PAGBs, which does not satisfy Brandon's criteria [14], were selected for the analysis of high angle boundaries. B segregation was quantified using three-dimensional atom probe (3DAP: LEAP-4000HR produced by CAMECA). Measurement temperature, pulse fraction and pulse rate for 3DAP analysis were 80 K, 20 % and 200 kHz, respectively. Although loss of Fe ions in detection of 3DAP measurement is known to cause overestimation of composition measurements [15], measured composition was not corrected because expected overestimation is as small as 10% in this measurement condition and detection loss of Fe ions inside of a grain boundary is unknown. Macroscopic B distribution and boride precipitation were analyzed by secondary ion mass spectroscopy (SIMS: TOF-SIMS5-100 produced by ION-TOF) with Bi^+ as a primary ion. Signals originated from B atoms are detected as BO_2^- in SIMS while its mass (m) is very close to other ions, AlO^- and $C_2H_3O^-$, $\Delta m / m < 0.0005$. Accordingly, mixing of signals from those ions makes understanding of SIMS data not-straightforward. Therefore, first, we optimized the observation condition using high mass-resolution mode so as signals of BO_2^- ion to be much higher than the other two ions. Then total signals of the three ions were acquired to make a map in high spatial resolution mode where mass resolution is not sufficient to distinguish signals of those three ions. The map will be denoted as BO_2^- map, hereafter.

Before quantitative measurement of B segregation, precipitation of boride in three specimens was investigated using SIMS because solubility of B in austenite is quite small and depends greatly on a temperature [16]. Fig. 2(a) shows a vertical section of a phase diagram of an Fe-0.2C-2Mn-B system calculated using ThermoCalc with a TCFE9 database. 1200 ^oC and 1150 ^oC are within austenite single phase region while 900 ^oC is slightly below solubility of Fe_2B. Figs. 2(b) and (c) show BO_2^- maps taken from the Q1050^{o}C and Q900^{o}C specimens, respectively. B segregation at PAGB is clearly seen in both specimens. In addition, boride precipitation is detected within austenite grain in the Q900^{o}C specimen.

To investigate B segregation without an influence by boride precipitation, the Q1200^{o}C specimen was selected and B segregation were measured at several PAGBs with different misorientation angles (θ). Figs. 3(a) and (b) show 3DAP results measured from low angle ($\theta = 10^o$) and high angle PAGBs ($\theta = 45^o$), respectively. Three dimensional maps in Figs. 3(a) and (b) clearly displays B and C segregation at the PAGBs. Element profiles across the PAGBs shows both B and C are enriched at

the PAGBs and segregation is enhanced at higher θ. It should be noted that carbon atoms forms cluster as indicated as red arrows, which may correspond to defects in martensite such as dislocations or lath boundaries, in accordance with previous 3DAP measurements [9, 10]. The formation of C clusters strongly indicates that C diffusion after martensite transformation changes C distribution in austenite. Since solubility of C in ferrite is much lower than that in austenite, C atoms are probably further segregated to prior austenite grain boundaries after martensite transformation, which makes quantitative investigation of grain boundary segregation of C in austenite state impossible. Amount of B segregation was evaluated as an interfacial excess, which is the number of solute atoms per unit area of a boundary [17], and plotted against θ in Fig. 3(c). B segregation increases with increasing θ up to 30° and becomes constant at higher θ.

Since grain boundary dependence is small at high angle boundary, effects of quenching temperature on B segregation was investigated only at high angle random PAGBs whose θ is larger than 30 °. Figs. 4(a) and (b) show three-dimensional B maps and element profiles across high angle PAGBs taken from the Q1050°C and Q900°C specimens, respectively. Compared with the Q1200°C specimen in Fig. 3(b), B segregation at PAGB becomes lower at lower quenching temperature. Fig. 4(c) summarizes an effect of the quenching temperature on B segregation at high angle PAGBs. The same symbols represent 3DAP dataset of different needle specimens taken from the same PAGB. It is clear that B segregation decreases with lowering quenching temperature. Precipitation of boride before quenching cannot be an only reason for this temperature dependency because boride precipitation was not observed at 1050°C (Fig. 1) and 1200 °C. The broken curve in Fig. 4(c) shows equilibrium B segregation at quenching temperature calculated using well-accepted segregation energy for B at austenite grain boundary [4], $x_B^{gb}/(1-x_B^{gb}) = x_B^{\gamma}/(1-x_B^{\gamma}) \exp\left(-\frac{0.65eV}{k_B T}\right)$, where x_B^{gb} and x_B^{γ} are B atomic-fraction in austenite grain boundaries and austenite matrix, respectively. B segregation site density per unit area of PAGB was assumed to be 48 site / nm^2 [10]. Measured B segregation is higher than the equilibrium segregation and the discrepancy increases at higher temperature. On the other hand, Takahashi et al. [10] developed a diffusion limited segregation model which considers equilibrium B segregation locally at austenite grain boundary and austenite matrix adjacent to grain boundary together with B diffusion in austenite matrix. They shows that their model can explain the amount of B segregation in the specimen cooled from 950°C at various cooling rates when boride precipitation is avoided [10]. B segregation during quenching at a cooling rate of 1000 °C/s was calculated using parameters they used and shown as a function of quenching temperature as a solid curve in Fig. 4(c). B segregation calculated by the diffusion limited model agrees well with that in the Q900°C specimen while the model cannot explain the inverse temperature dependency observed in the Q1050°C and Q1200 °C.

Site-competition between B and C atoms is possible mechanism causing the inverse temperature

dependency of B segregation. Suzuki et al. [18] show that segregation of solute atoms with weaker segregation energy is reduced at lower temperature because segregation sites are dominantly occupied by the other solute atoms with stronger segregation energy. B has stronger segregation energy (0.65eV [4]) than C (0.31eV [19]) to austenite grain boundaries so that site-competition between B and C cannot rationalize the inverse temperature dependency of B observed in this study. Co-segregation of B and C may induce excess segregation of B than equilibrium segregation, however, it cannot induce the inverse temperature dependency.

Accordingly, the observed inverse temperature dependence strongly suggests large influence of non-equilibrium B segregation during quenching from high temperature. In this mechanism, it is assumed that a part of vacancy forms complex with B atom in solution due to attractive interaction between them [20] and absorption of excess vacancies at austenite grain boundaries induces a flow of the vacancy-B complex to austenite grain boundaries, resulting in excess enrichment of B at austenite grain boundaries.

Vacancy concentrations in austenite estimated by $4.5exp\left(-\frac{1.4eV}{kT}\right)$[21, 22] are 4.3, 21, 73 at-ppm at 900, 1050, 1200 ^{o}C, respectively and vacancy concentration at 1200 ^{o}C is comparable with B concentration in this alloy, namely 56 at-ppm B. Furthermore, a diffusion distance of vacancy in austenite during quenching was calculated using a diffusion parameter of vacancy in austenite [21] and 1000 ^{o}C/s for the cooling rate. It is 7.2μm for quenching from 1200^{o}C, which is about 5 times longer than that for the quenching from 900 ^{o}C. Therefore, more excess vacancies with longer diffusion distance should enhance non-equilibrium segregation of B during quenching from 1200 ^{o}C compared with quenching from 900 ^{o}C. Accurate parameterization of diffusivity of complex, binding energy between B and vacancy and segregation energy of complex to grain boundary will be needed to develop a segregation model, which takes effects of vacancy and vacancy-B complex on segregation into account in future.

It is well known that more solute is segregated at high angle random grain boundaries than that for low angle grain boundaries or CSL boundaries [11]. Herbig et al. [12] reported that C segregation to ferrite low angle boundaries is lower than that at high angle random boundaries. They supposed that C atoms are absorbed to dislocation cores in the low angle boundaries unlike to C segregation to high angle random grain boundaries. Similarly, present study first reported that B segregation at austenite grain boundary is reduced at low angle grain boundaries. Because observed B segregation is much higher than the equilibrium segregation as shown in Fig. 4(c), misorientation dependency not in equilibrium segregation but in non-equilibrium segregation should cause the misorientation dependency observed. High angle random boundaries are more effective sink for vacancies than low angle grain boundaries consisting of dislocations so that a vacancy-B complex flow to high angle

boundaries should be more extensive than that to low angle grain boundaries, which may result in the misorientation dependency in non-equilibrium segregation.

In summary, segregation of B atoms at random austenite grain boundaries was investigated quantitatively using 3DAP. B segregation increases with increasing temperature before quenching, which suggests that non-equilibrium segregation occurs during quenching especially at higher quenching temperature. B segregation at austenite grain boundary is reduced at low angle random boundaries than high angle random grain boundaries, probably due to difference in ability to absorb excess vacancies between low and high angle boundaries.

The authors greatly appreciate contributions by Ms. Rie Shishido in IMRAM, Tohoku University and Mr. Kunio Shinbo in IMR, Tohoku University for SIMS and 3DAP measurements, respectively.

Reference

[1] F. B. Pickering : Physical Metallurgy and the Design of Steels, Applied Science Publishers LTD, London, (1978) 103-104.

[2] J.E. Morral, T.B. Cameron, Met. Trans. A, 8A (1977), 1817-1819.

[3] L. Karlsson, H. Norden, H. Odelius, Acta Metall. 36 (1988), 1-12.

[4] L. Karlsson, H. Norden, Acta Metall. 36 (1988), 13-24.

[5] X.L. He, Y.Y. Chu, J.J. Jonas, Acta Metall., 37 (1989), 2905-2916.

[6] X.L. He, Y.Y. Chu, J.J. Jonas, Acta Metall., 37 (1989), 147-161.

[7] R.G.Faulkner, J. Mater. Sci. 16 (1981), 373-383.

[8] G. Shigesato, T. Fujishiro, T. Hara, Metall. Mater. Trans. A, 45 (2014), 1876-1882.

[9] Y.J. Li, D. Ponge, P. Choi, D. Raabe, Ultramicroscopy, 159(2015), 240-247.

[10] J. Takahashi, K. Ishikawa, K. Kawakami, M Fujioka, N. Kubota, Acta Mater., 133(2017), 41-54.

[11] P. Lejček, Grain boundary segregation in metals, Springer, 2010

[12] M. Herbig, D. Raabe, Y. J. Li, P. Choi, S. Zaefferer, and S. Goto, Phys. Rev. Lett., 112 (2013), 126103-1-5

[13] G.Miyamoto, N.Iwata, N.Takayama, T.Furuhara, Acta Mater., 58(2010), 6393-6403.

[14] D.G. Brandon, Acta Metall., 14(1966), 1479-1484.

[15] G.Miyamoto, K. Shimbo, T.Furuhara, Scripta Mater., 67(2012), 999-1002.

[16] T. B. Cameron and J. E. Morral, Metal. Trans. A, 17 (1986), 1481-1483

[17] B.W. Krakauer, D. N. Seidman, Phys. Rev. B 48(1993), 6724–6727.

[18] S. Suzuki, M. Obata, K. Abiko, H. Kimura, Scr. Metall., 17(1983), 1325-1328.

[19] M. Paju, H. Viefhaus, H.J. Grabke, Steel Research, 59(1988), 336-343

[20] T.M. Williams, A.M. Stoneham, D.R. Harries, Met. Sci., 10 (1976). 14-19.

[21] L. Karlsson, Acta Metall. 36 (1988), 25-34.

[22] A.D. Brailsford, R.D. Bullough, J. Nucl. Mater. 44 (1972) 121-135.

Figure(s)

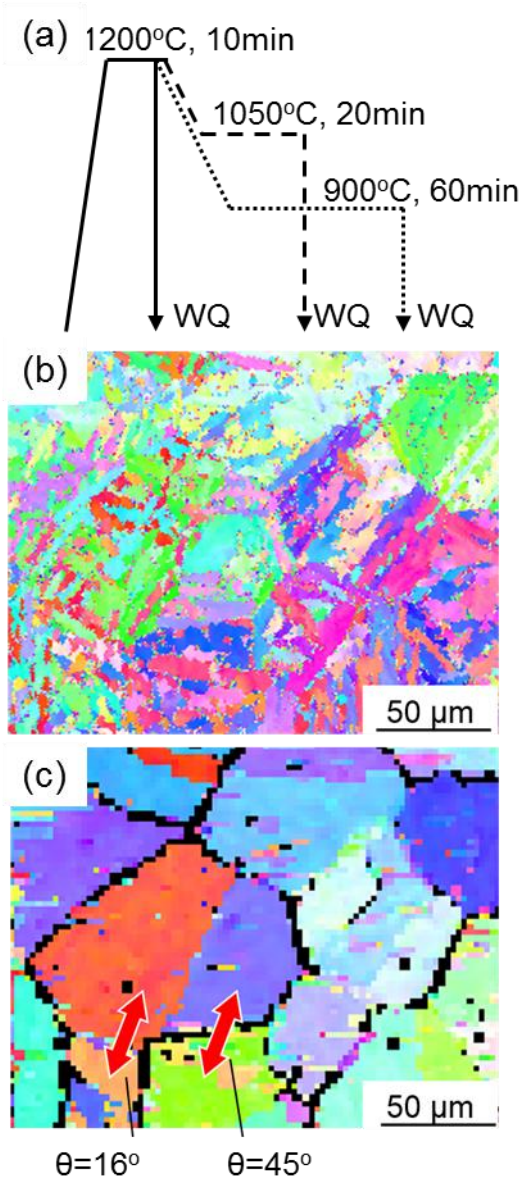

Figure 1 (a) Heat treatment conditions used in this study, (b) orientation map of martensite, (b) austenite orientation map reconstructed from (a). θ represent misorientation angle of austenite grain boundary.

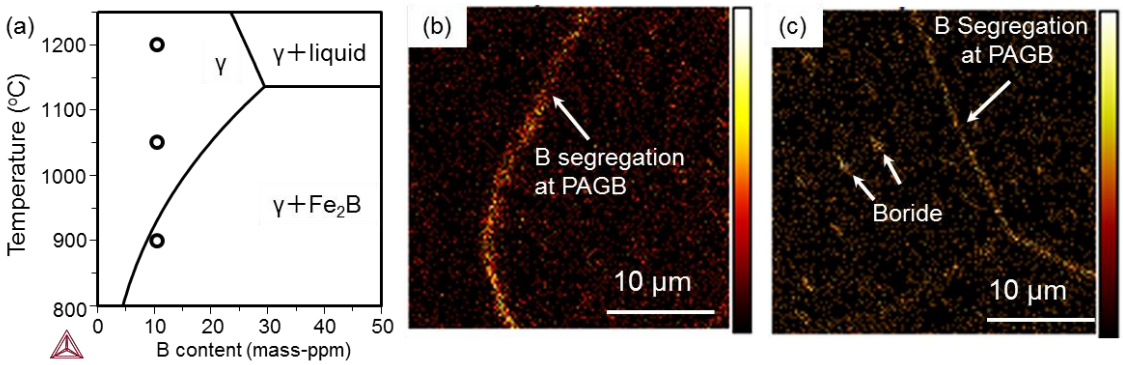

Figure 2 (a) Vertical section of a phase diagram of Fe-2Mn-0.2C-B system, and BO_2^- maps from (b) Q1050°C and (c)Q900 °C specimens. Circles in (a) represent quenching temperatures used in this study.

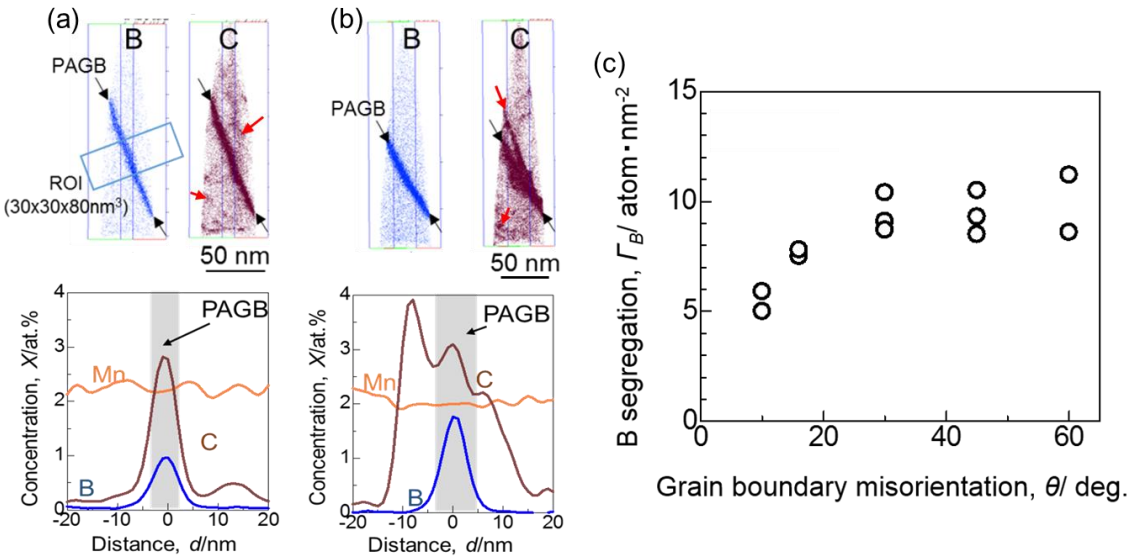

Figure 3 Three dimensional maps of B and C and corresponding solute content profiles across random PAGB with misorientations of (a) $\theta = 10^{o}$ and (b) $\theta = 45^{o}$ in the Q1200°C specimen, (c) amount of B segregation as a function of θ in the Q1200°C specimen. Red arrows in C maps in (a) and (b) indicate C cluster or segregation at defects in martensite structures.

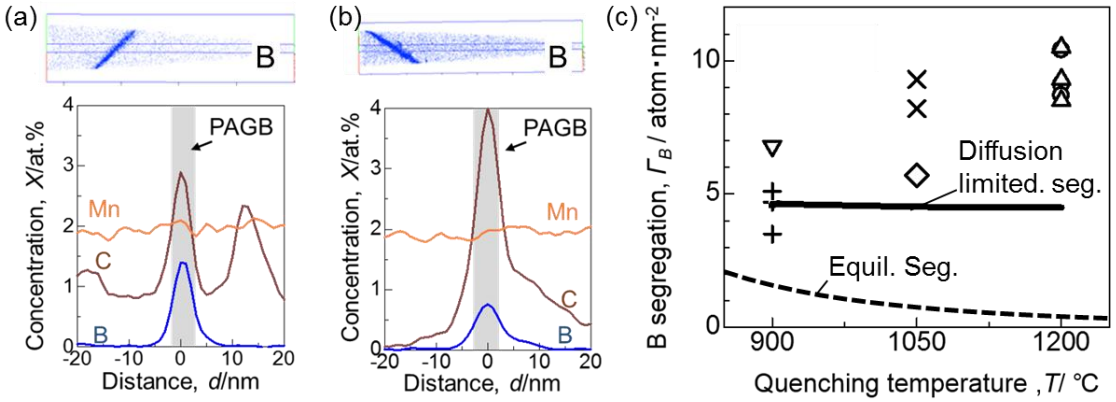

Figure 4 Three dimensional maps of B and C and corresponding solute content profiles across high angle PAGB in (a) Q1050^{o}C (θ = 45^{o}), (b) Q900^{o}C specimens (θ = 45^{o}), (c) B segregation at high angle PAGB as a function of quenched temperature. The same symbols in (c) represent 3DAP dataset of different needle specimens taken from the same PAGB. Broken and solid curves display variations of B segregation with quenching temperature calculated by the equilibrium segregation model and B segregation calculated by the diffusion limited segregation model after quenching, respectively.

*Graphical Abstract